iScience

CellPress
OPEN ACCESS

Article

Ablation of collagen XII disturbs joint extracellular matrix organization and causes patellar subluxation

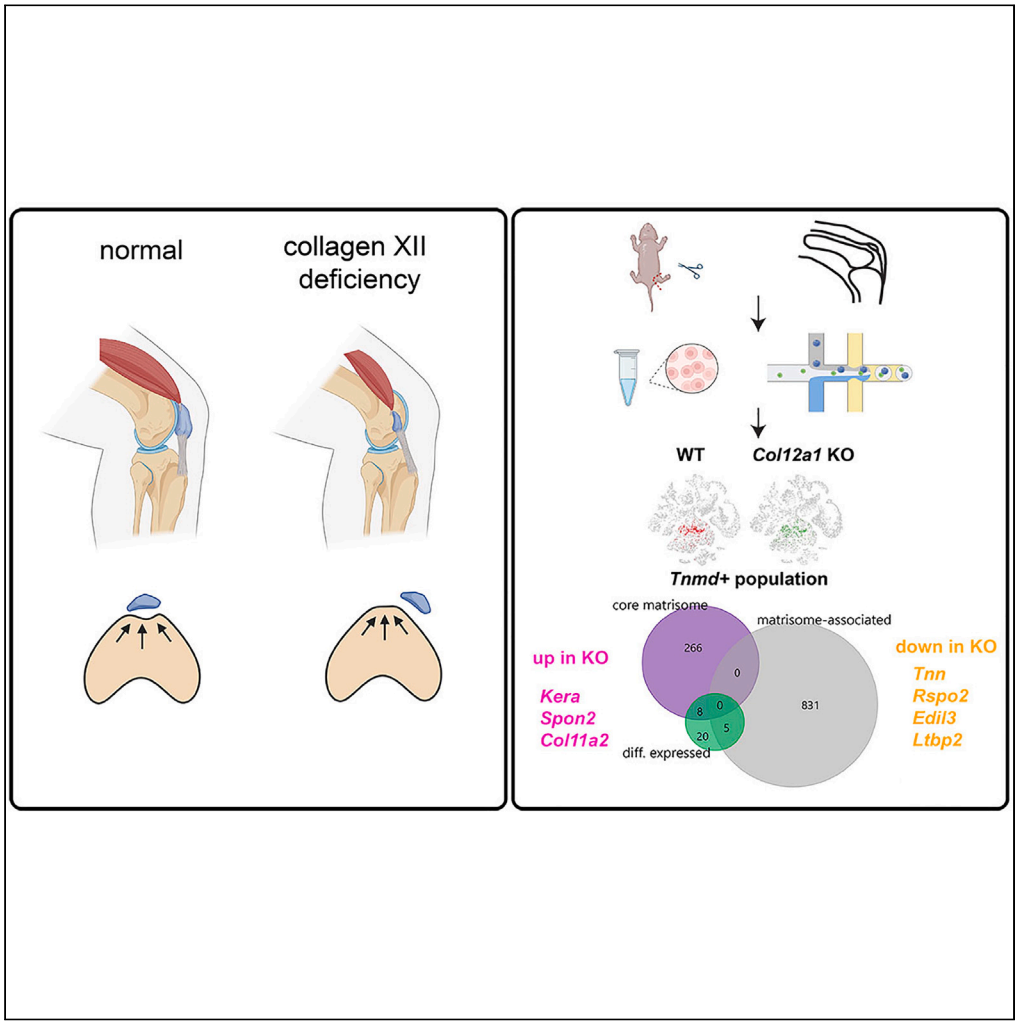

Mengjie Zhu, Fabian Metzen, Mark Hopkinson, ..., Mats Paulsson, Manuel Koch, Bent Brachvogel

manuel.koch@uni-koeln.de (M.K.)
bent.brachvogel@uni-koeln.de (B.B.)

Highlights

Collagen XII is widely expressed in connective tissues of the patellofemoral joint

Lack of collagen XII causes patellar subluxation and quadriceps muscle degeneration

Collagen XII is crucial to stabilize the joint extracellular matrix in mice and in humans

Zhu et al., iScience 26, 107225
July 21, 2023
https://doi.org/10.1016/j.isci.2023.107225

iScience

CellPress
OPEN ACCESS

Article

Ablation of collagen XII disturbs joint extracellular matrix organization and causes patellar subluxation

Mengjie Zhu,[1,2,3] Fabian Metzen,[2,3] Mark Hopkinson,[4] Janina Betz,[2,3] Juliane Heilig,[5,7] Jassi Sodhi,[6] Thomas Imhof,[2,3] Anja Niehoff,[5,7] David E. Birk,[8] Yayoi Izu,[9] Marcus Krüger,[10,17] Andrew A. Pitsillides,[4] Janine Altmüller,[11,12,13] Gerjo J.V.M. van Osch,[14,15] Volker Straub,[6] Gudrun Schreiber,[16] Mats Paulsson,[3,17] Manuel Koch,[2,3,17,*] and Bent Brachvogel[1,3,18,*]

SUMMARY

Collagen XII, belonging to the fibril-associated collagens, is a homotrimeric secreted extracellular matrix (ECM) protein encoded by the *COL12A1* gene. Mutations in the human *COL12A1* gene cause an Ehlers-Danlos/myopathy overlap syndrome leading to skeletal abnormalities and muscle weakness. Here, we studied the role of collagen XII in joint pathophysiology by analyzing collagen XII deficient mice and human patients. We found that collagen XII is widely expressed across multiple connective tissue of the developing joint. Lack of collagen XII in mice destabilizes tendons and the femoral trochlear groove to induce patellar subluxation in the patellofemoral joint. These changes are associated with an ECM damage response in tendon and secondary quadriceps muscle degeneration. Moreover, patellar subluxation was also identified as a clinical feature of human patients with collagen XII deficiency. The results provide an explanation for joint hyperlaxity in mice and human patients with collagen XII deficiency.

INTRODUCTION

Extracellular matrix (ECM) and, in particular, collagens play an important role in the musculoskeletal system. Collagen XII, a homotrimer which belongs to the subfamily of fibril-associated collagens with interrupted triple helices (FACIT), is widely expressed in mice and humans, e.g. in skin, cartilage, nerve, and muscle.[1] In most tissues, collagen XII is associated with collagen fibrils but also with tenascin-X.[2,3] Collagen XII occurs in several splice variants of which the largest is a 300 kDa protein (18 FN3, 4 VWA, 1 TSPN, and 2 COL domains), whereas the short splice variant lacks a large part of the N-terminal region.[4] The larger form contains an additional heparin binding site in the 7th FN3 domain; moreover glycosaminoglycan chains are covalently attached. Collagen XII has been identified as a key collagen of the ECM in tendon, bone, cornea, and muscle.[1] Mutations in the *COL12A1* gene were identified as the cause of myopathic Ehlers-Danlos (mEDS) overlap syndrome.[5,6] Depending on the nature of the mutation, dominant or recessive, the phenotype varies in severity.[7] Patients with a homozygous loss of function mutation show joint hyperlaxity combined with weakness precluding independent walking and feeding as newborn.[8] Owing to night-time hypoventilation, noninvasive night-time ventilation may be required. Severe kyphoscoliosis is another hallmark of mEDS. Of interest, the muscle weakness is not progressive and patients with *de novo* missense mutations are more mildly affected. Surprisingly, the muscle weakness and the ability to walk improve over time.[5,6]

Collagen XII deficient (*Col12a1* KO) mice recapitulate the phenotype observed in *COL12A1* deficient patients.[6] However, as often observed for ECM genes, the phenotypes in mice are less severe and, in the case of *Col12a1* KO mice, the mice can feed by themselves and are able to walk postnatally. Analysis of the bones from KO mice revealed a brittle bone phenotype because of a lack of osteoblast polarity.[9] Of interest, osteocytes have fewer dendritic extensions, which may affect fiber domain organization and cause abnormal fiber packing. Detailed morphological analysis of different tendons revealed that 20–60% of the KO mice display discontinuity in the anterior, but not in the posterior cruciate ligament and have an increased risk of anterior cruciate ligament injury.[10] These studies show that collagen XII is crucial for

Continued

[1]Department of Pediatrics and Adolescent Medicine, Experimental Neonatology, Faculty of Medicine and University Hospital Cologne, University of Cologne, Cologne, Germany

[2]Institute for Dental Research and Oral Musculoskeletal Biology, Faculty of Medicine and University Hospital Cologne, University of Cologne, Cologne, Germany

[3]Center for Biochemistry, Medical Faculty and University Hospital Cologne, University of Cologne, Cologne, Germany

[4]Skeletal Biology Group, Comparative Biomedical Sciences, The Royal Veterinary College, Royal College Street, London, UK

[5]Institute of Biomechanics & Orthopaedics, German Sport University Cologne, Cologne, Germany

[6]John Walton Muscular Dystrophy Research Centre, Translational and Clinical Research Institute, Faculty of Medical Sciences, Newcastle University and Newcastle Hospitals NHS Foundation Trust, Newcastle, UK

[7]Center for Musculoskeletal Biomechanics (CCMB), Medical Faculty and University Hospital Cologne, University of Cologne, Cologne, Germany

[8]College of Medicine, University of South Florida, Morsani, Tampa, FL, USA

[9]Department of Veterinary Medicine, Okayama University of Science, Ehime, Japan

[10]Institute of Genetics and Cologne Excellence Cluster on Cellular Stress Responses

ECM integrity in bone and tendon but the consequences for joint stability and function are poorly understood.

Here, we address the physiological roles of collagen XII in knee joint organization. We define the localization of collagen XII in the developing joint, study the consequences of loss of collagen XII for joint stability and, by snRNA-seq, define the molecular changes occurring on loss of collagen XII in tenocytes. Finally, we transfer our findings to humans and identify a novel clinical feature in patients with mEDS overlap syndrome.

RESULTS

Collagen XII is widely expressed in connective tissues during postnatal joint development

We first determined collagen XII localization in bone, cartilage, tendons, and ligament joint tissues during postnatal development. Collagen XII was detected by immunofluorescent staining in whole hindlimb knee joint sections from infant (postnatal P3, P7) and juvenile (1 month) mice. A strong collagen XII signal was apparent in patella, articular cartilage, quadriceps tendon, periosteum of the femur of infant mice (Figure 1A) and a weak signal in the muscle basement membrane. In juvenile mice, collagen XII was hardly found in the patella and articular cartilage, but is still present in tendons and ligaments. In synovial joints, collagen XII was localized in the anterior and posterior cruciate ligaments and in the articular cartilage of femur and tibia (Figure 1B). Collagen XII was also detected in the enthesis, where the patella tendon attaches to the tibial plateau and in the periosteum of the tibia (Figure 1C). The results show that collagen XII is found in the patella-tendon-ligament unit, presumably contributing to the transmission of mechanical forces and to maintaining joint stability.

Collagen XII deficiency causes patellar subluxation

A *Col12a1* KO mouse model was then used to study the consequences of collagen XII deficiency for the structural tissue organization and functional integrity of joints *in vivo*. This model was generated by targeted deletion of exon 2–5, as described previously.[9] The absence of collagen XII was confirmed by immunofluorescent analysis of whole hindlimb knee joint sections from infant and juvenile mice (see Figure S1). The mice showed growth retardation (see Figures S2A and S2B), a delay in secondary ossification center formation at P7 and P12, shorter bones (see Figures S2C and S2E) and, most strikingly, an abnormal appearance of the stifle joint in adult mice (Figure 2A). µCT analysis was performed to visualize the three-dimensional organization of bony elements in the distal hindlimb joints of 1-month-old wild type (WT) and *Col12a1* KO mice. In line with previous findings, a decrease in trabecular bone mass was observed (Figure 2B, see also Figure S2F). In addition, 3 out of 4 *Col12a1* KO mice had a delocalized patella, outside of the femoral trochlear groove. This patellar subluxation was never detected in WT mice. Next, histological analysis with H&E and Alcian blue staining of joint sections was applied to study patellar subluxation during postnatal development. At P3 and P7 *Col12a1* KO mice are barely mobile and here patellar subluxation was detected in only 20% (P3 - 2/10) and 30% (P7 - 3/10), respectively. At P12, when mice begin to move and generate significant mechanical forces through muscle contraction, patellar subluxation was found in 67% of the *Col12a1* KO mice (4/6), but not in WT mice (0/6). This was also evident in 1-month-old mice, whereas 75% (6/8) *Col12a1* KO mice showed patellar subluxation (Figures 2C and 2D). The data suggest that increased muscle forces during later postnatal development result in patellar subluxation because of the destabilization of patella-tendon-ligament unit.

Patellar subluxation results in secondary muscle degeneration

Patellar subluxation results in a dysfunctional joint but may also impair muscle function. Of interest, a profound reduction in *Musculus (M.) quadriceps femoris* muscle mass was found in older postnatal (P12), juvenile (1 month) and adult (6 months) *Col12a1* KO mice compared to WT littermates, but not in P3 mice (Figure 3A). To determine whether the loss of muscle mass is specific for the quadriceps and because of patellar subluxation, we compared muscle mass and nuclear position in fibers of *M. quadriceps femoris* and *M. gastrocnemius* in 6-month-old mice. After being normalized to body weight, both *M. quadriceps femoris* mass (WT: 0.72 ± 0.19% vs. KO: 0.51 ± 0.05%, mean ± SD) and *M. gastrocnemius* muscle mass (WT: 0.56 ± 0.06% vs. KO: 0.41 ± 0.09%; mean ± SD) were significantly decreased in *Col12a1* KO mice (Figure 3B). H&E staining on cross-sections was then used to study the organization of muscle fibers (n = 10 samples per group). An increased number of centralized nuclei was detected in *M. quadriceps femoris*

in Aging-Associated Diseases (CECAD), University of Cologne, Cologne, Germany

[11]Cologne Center for Genomics, University of Cologne, Cologne, Germany

[12]Berlin Institute of Health at Charité, Core Facility Genomics, Berlin, Germany

[13]Max Delbrück Center for Molecular Medicine in the Helmholtz Association, Berlin, Germany

[14]Department of Orthopaedics and Sports Medicine, Erasmus MC, University Medical Center, Rotterdam, the Netherlands

[15]Department of Otorhinolaryngology, Erasmus MC, University Medical Center, CN Rotterdam, the Netherlands

[16]Department of Neuropediatrics, Klinikum Kassel, Kassel, Germany

[17]Center for Molecular Medicine Cologne (CMMC), University of Cologne, Cologne, Germany

[18]Lead contact

*Correspondence: manuel.koch@uni-koeln.de (M.K.), bent.brachvogel@uni-koeln.de (B.B.)

https://doi.org/10.1016/j.isci.2023.107225

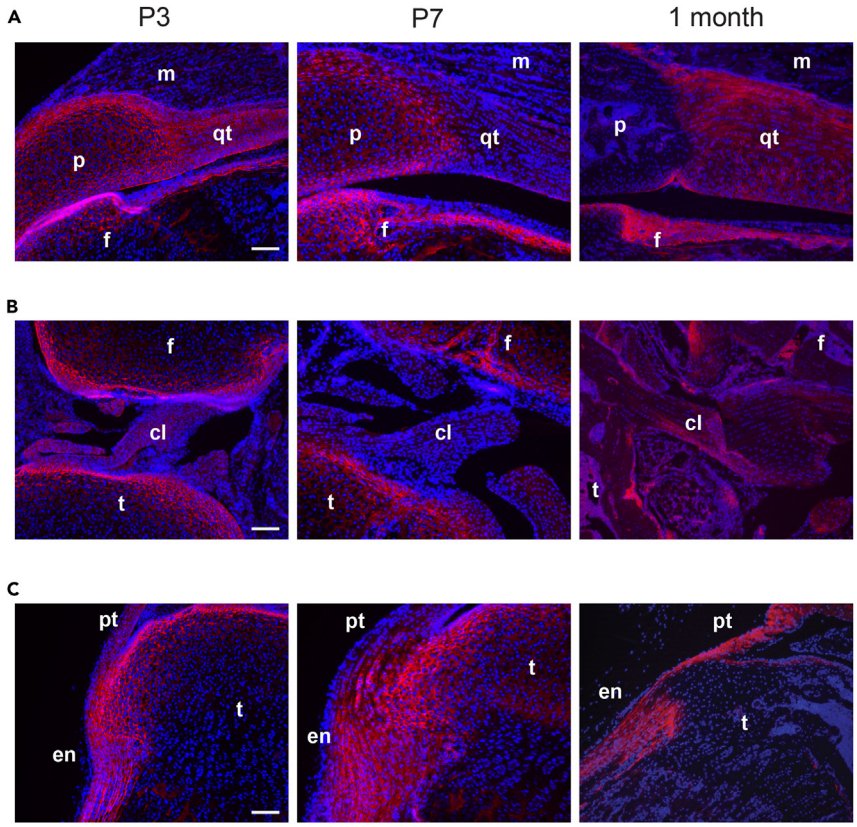

Figure 1. Collagen XII is expressed during murine musculoskeletal system development

(A) Localization of collagen XII was analyzed by immunofluorescent staining using sections from whole hindlimb knee joints of P3, P7 and 1-month-old mice. Collagen XII (red) detection in patella (p), patella-tendon (pt), femur (f), tibia (t) cartilage, cruciate ligament (cL), quadriceps tendon (qt), enthesis (en), and muscle (m). Cell nuclei are counterstained with DAPI (blue).

(B and C) Images of collagen XII expression in (B) synovial joint and (C) enthesis. A–C Scale bar: 100 μm.

(WT: 0.40 ± 0.19% vs. KO: 2.4 ± 0.46%, mean ± SD) and *M. gastrocnemius* (WT: 0.66 ± 0.24% vs. KO: 2 ± 0.95%, mean ± SD) *in Col12a1* KO mice (Figures 3C and 3D).

In addition, cross sections were stained with wheat germ agglutinin (WGA) to determine the distance between the WGA+ cell membranes of a single myofiber (see Figure S3). The minimum Feret's diameter of individual WGA+ myofibers was analyzed using the Mysoft tool utilizing the FIJI/ImageJ software.[11] *M. quadriceps femoris* of *Col12a1* KO mice exhibited increased numbers of myofibers with the diameter of 0–30 μm (WT: 0.34 ± 0.15% vs. KO 0.62 ± 0.18%, mean ± SD), 30–40 μm (WT: 6.98 ± 1.15% vs. KO 8.74 ± 1.10%, mean ± SD), >80 μm (WT: 12.89 ± 4.40% vs. KO 17.12 ± 3.01%, mean ± SD) and decreased number of myofibers in the range of 60–70 μm (WT: 22.28 ± 1.47% vs. KO 19.03 ± 1.06%, mean ± SD) as compared to WT littermates (Figure 3E, upper panel). In *M. gastrocnemius*, less myofiber numbers were only detected at the diameter range of 60–70 μm (WT: 22.64 ± 2.82%; KO, 20.13 ± 2.40%, mean ± SD) in *Col12a1* KO mice compared to control (Figure 3E, lower panel). Hence, patellar subluxation in *Col12a1* KO mice results in a secondary loss of femoral muscle mass, in centralized nuclei and in a shift toward enlarged quadriceps muscle fibers because of joint dysfunction.

The femoral trochlear groove is altered in collagen XII deficient mice

The patella sits in the trochlear groove of the distal femur to prevent its subluxation in the patellofemoral joint. We therefore studied the organization of the femoral trochlear groove in late postnatal *Col12a1* KO mice (P7), when a high incidence of patella dislocation was first evident. Lugol's solution was used to visualize soft tissue in X-ray based μCT scanning of these hind limb joints. The original data were reconstructed to disclose the femur (gray), the *M. rectus femoris* of the *M. quadriceps femoris* group

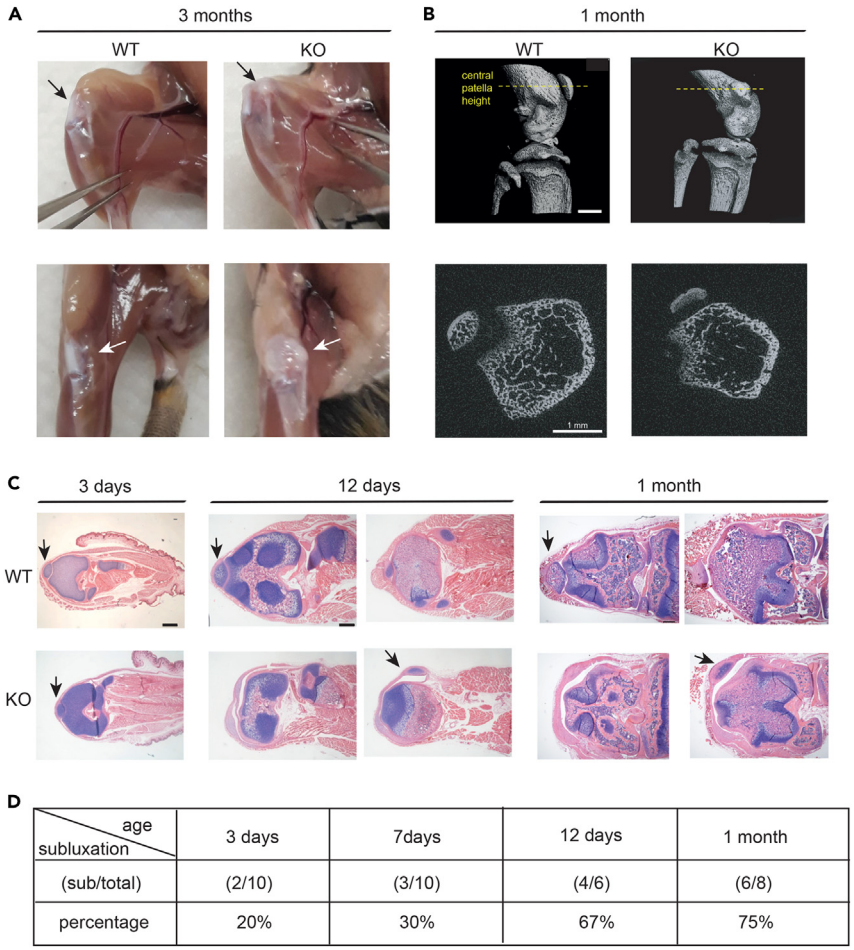

D

age / subluxation	3 days	7days	12 days	1 month
(sub/total)	(2/10)	(3/10)	(4/6)	(6/8)
percentage	20%	30%	67%	75%

Figure 2. *Col12a1* KO mice develop patellar subluxation

(A) Images representing anterior-posterior views of 3-month-old WT and *Col12a1* KO mouse hindlimb knee joints after skin removal.

(B) Representative μCT images from 1-month-old WT and KO mouse hindlimb knee joints (n = 4 samples per group, see also Figure S2F). Scale bar: 1 mm.

(C) In plane-matched paraffin sections from WT and *Col12a1* KO mice were stained with hematoxylin (nuclei, purple), eosin (cytoplasm, pink) and Alcian blue (proteoglycans, blue). Arrows indicate patella location. Scale bar: 500 μm.

(D) Quantification of patellar subluxation rate in *Col12a1* KO mice of different ages. Percentages are given.

(green), the patella and the surrounding ligament (red). This showed subluxation of the KO patella (Figure 4A). Volume renderings of μCT data often revealed flattened or convex surfaces at the femoral trochlear grooves in *Col12a1* KO mice (Figure 4B), whereas those of WT were well-formed and appeared to have concave surfaces (see also Figure S4). The *Col12a1* KO group displays a reduced volume of the *M. rectus femoris* compared to WT (WT: 2.79 ± 0.46 mm^3 vs. KO 1.26 ± 0.08 mm^3, mean ± SD) (Figure 4C) and a significantly shorter perimeter and smaller cortical bone area at the mid-shaft of the femur (Figure 4D). The results indicate that the lack of femoral trochlear grooves in *Col12a1* KO mice may favor the dislocation of the patella and, secondarily, affects *M. quadriceps femoris* muscle organization.

Collagen XII deficiency results in transcriptional responses of ECM-related genes

snRNA-seq was applied to define transcriptional responses in individual cell populations after patella dislocation and joint immobilization. Single cell suspensions were obtained by collagenase digestion of hindlimb knee joints from WT and *Col12a1* KO mice (P7) (Figure 5A). After library construction and cellular barcode labeling, massive parallel sequencing was performed in two independent experiments (1st experiment 1xWT vs. 1x *Col12a1* KO sample; 2nd experiment 2x WT vs. 2x *Col12a1 KO* samples) and then

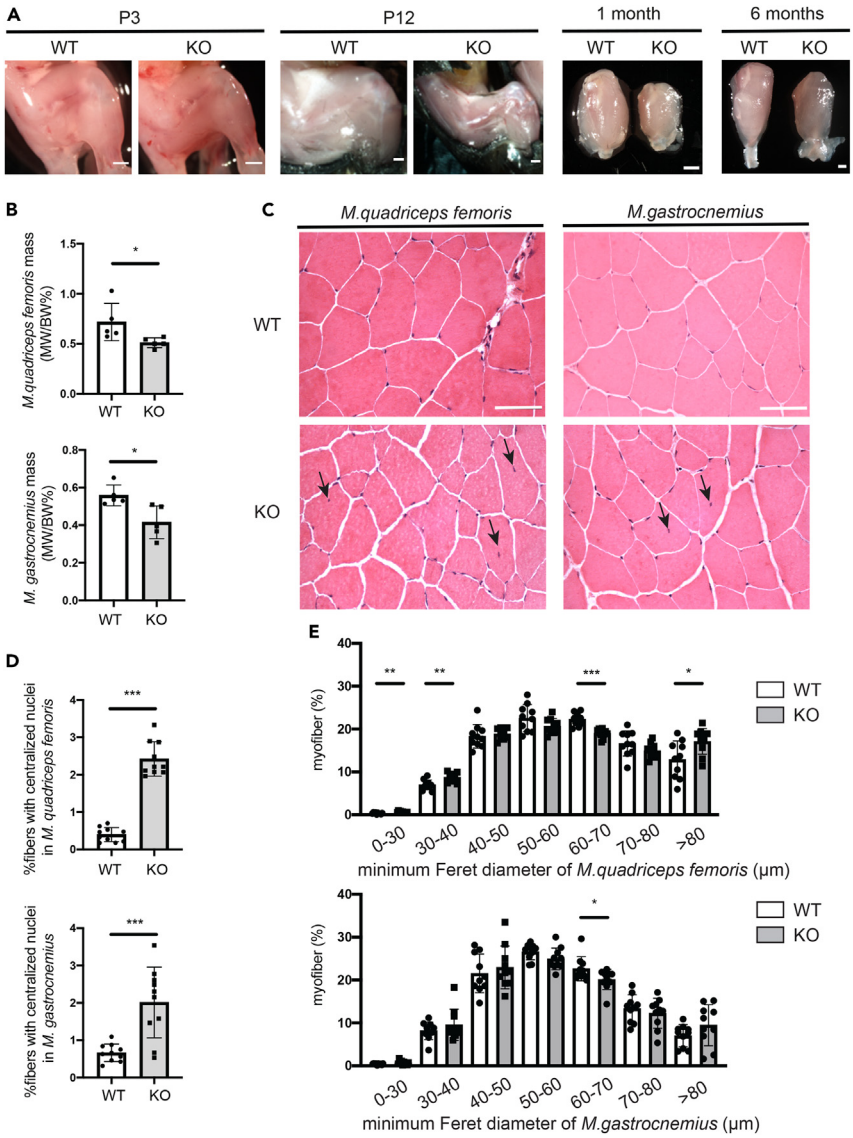

Figure 3. *Col12a1* KO mice show alterations in muscle fibers organization

(A) Representative images of the whole hindlimb knee joints from P3 and P12 mice after skin removal and of isolated quadriceps muscle from 1-month to 6-month mice. Scale bar, 1mm.

(B) *M. quadriceps femoris* and *M. gastrocnemius* were isolated from 6-month-old female mice and their weight (MW) normalized to individual body weight (BW) was quantified (n = 5 samples per group).Unpaired two-tailed Student's *t* test, *, $p < 0.05$. Error bars are mean ± SD.

(C) In plane matched 7 μm cryo-cross sections of *M. quadriceps femoris* and *M. gastrocnemius* muscle from 6-month-old WT and *Col12a1* KO mice (n = 10 samples per group) were stained with hematoxylin (nuclei, purple) and eosin (cytoplasm, pink). Representative images are shown. Scale bar, 100 μm. Black arrows indicate centralized nuclei.

(D) Percentage of myofibers with central nuclei was determined in *M. quadriceps femoris* and *M. gastrocnemius* muscles of both WT and *Col12a1* KO female mice at the age of 6 months (n = 10 samples per group). The percentage of myofibers with centralized nuclei is given. Unpaired two-tailed Student's *t* test, ***, $p < 0.001$. Error bars are mean ± SD.

(E) The percentage of individual WGA+ myofibers with a defined Feret's diameter was determined in *M. quadriceps femoris* and *M. gastrocnemius* muscle in WT and *Col12a1* KO female mice at the age of 6 months (n = 10 samples per group). Unpaired two-tailed Student's *t* test, *, $p < 0.05$; **, $p < 0.01$, ***, $p < 0.001$. Error bars are mean ± SD.

a combined dataset (n = 3 per genotype) was analyzed using the cell loupe browser. Quality assessment of the normalized dataset showed that an estimated 24203 cells (WT sample: 12297 cells, *Col12a1* KO sample: 11906 cells) with 7288 median UMI counts and 1484 median genes per cell were detected (see

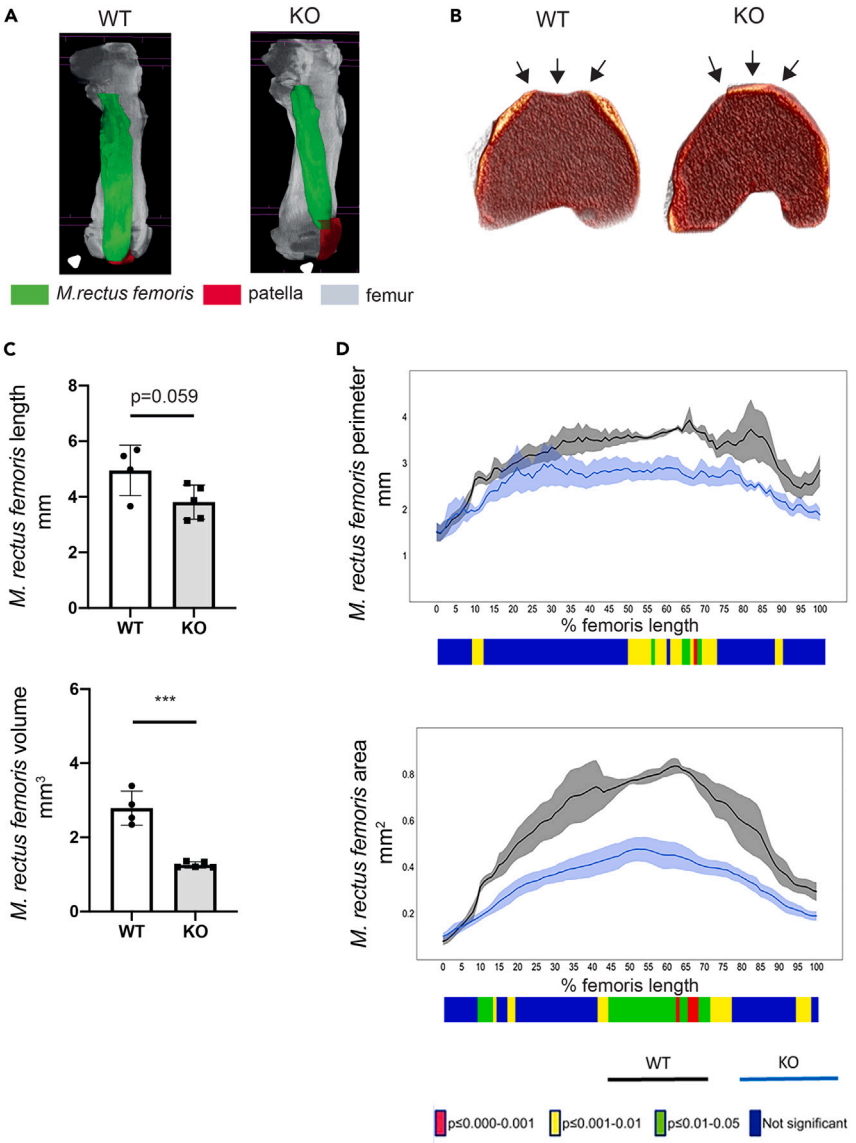

Figure 4. *Col12a1* KO mice show a malformed femoral trochlear groove and *M. rectus femoris* alterations at P7

(A) Representative images of μCT volume renderings of femora (gray), *M. rectus femoris* (green), patella and ligament (red) from P7 old WT and *Col12a1* KO mice.

(B) Representative images of μCT volume renderings of femora from WT and *Col12a1* KO mice. Arrows point at the femoral trochlear groove, malformed in KO (n = 4 samples for WT group, n = 5 samples for KO group, see Figure S4).

(C) μCT 3D morphometric analysis shows decreased length and volume of *M. rectus femoris* in P7 old *Col12a1* KO mice (n = 4 samples for WT group, n = 5 samples for KO group). Unpaired two-tailed Student's *t* test, ***, $p < 0.001$. Error bars are mean ± SD.

(D) μCT 2D morphometric analysis along the length of the Lugol's stained *M. rectus femoris* from 0% (proximal end) to 100% (distal end) show differences between the *Col12a1* KO group (n = 5 samples) when compared to the WT group (n = 4 samples) in muscle perimeter and muscle area. Line graphs represent the means ± SEM. Unpaired two-tailed Student's *t* test was used to compare means between WT and *Col12a1* KO groups. The graphical heatmap displays statistical differences at specific matched locations along the length of the femur. Red $p \leq 0.000–0.001$, yellow $p \leq 0.001–0.01$, green $p \leq 0.01–0.05$ and blue $p \geq 0.05$.

Figure S5). Individual cell cluster annotation by cell type-specific marker gene expression[12] in the combined (WT + KO) t-SNE plot was used to identify *Col2a1+* chondrocytes (cluster 1), *Col1a1+* mesenchymal cells (cluster 2) and *Tnmd+* tenocyte-like cells (cluster 3) within the dataset (Figure 5B). In WT mice a high *Col12a1* expression level (cluster 4) was found mainly in tenocytes and chondrocytes. The results confirm

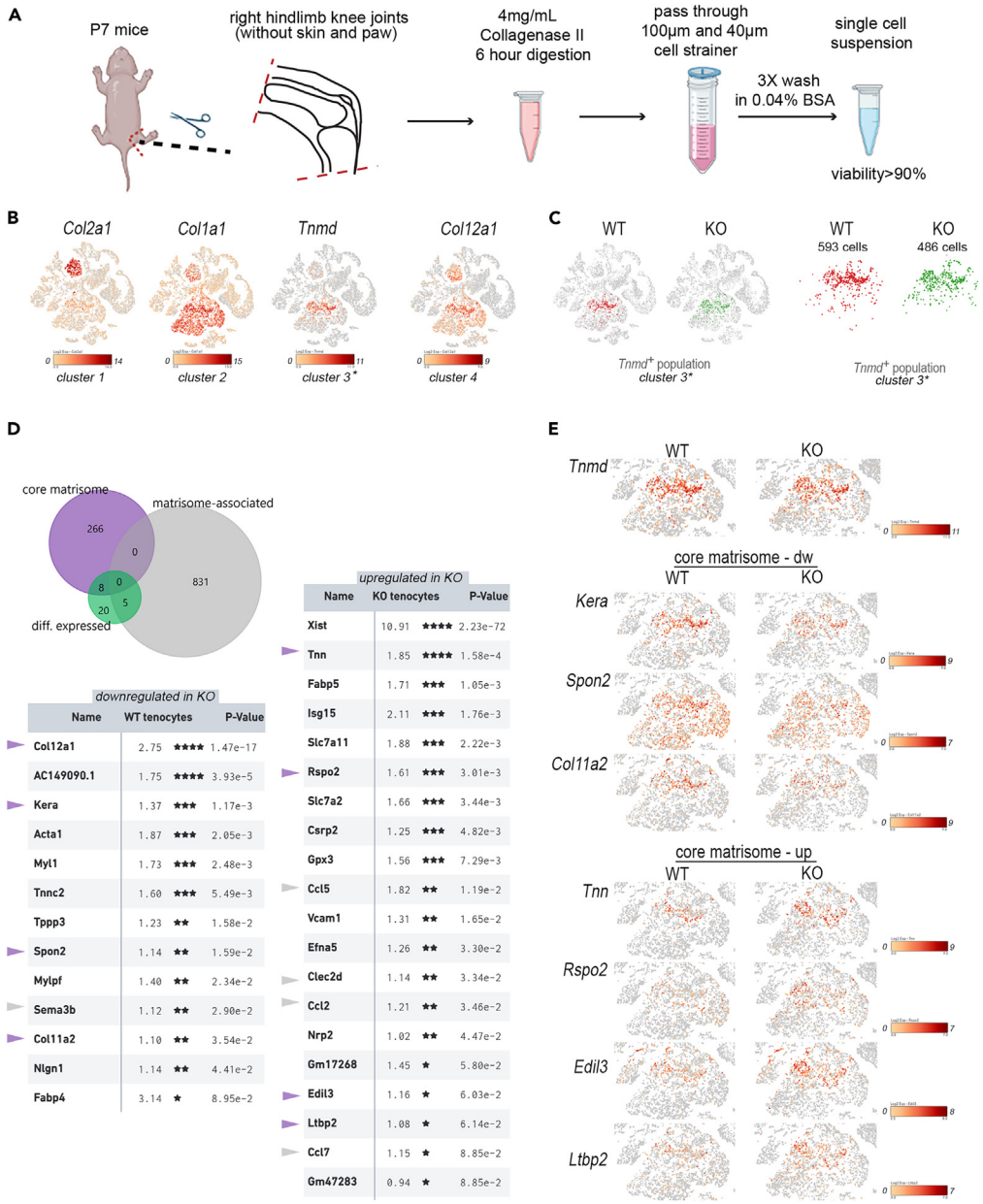

Figure 5. Combined scRNA-seq and matrisome analysis of the *Tnmd+* cell subpopulation

(A) Diagram of sample preparation for single cell sequencing. This figure is created with Biorender.com.

(B) Expression of cell type specific marker genes was used to annotate 4 different cell clusters. Log2 expression intensity values of individual genes are indicated in t-SNE plots (color scale).

(C) Tenocyte (*Tnmd*+) cell clusters (cluster 3) are shown in t-SNE plots and after gating.

(D) The proportions of differentially expressed entities within the core matrisome or matrisome associated cluster are shown in a Venn diagram. Genes that are down-or upregulated in tenocytes from *Col12a1* KO are listed. Log2 fold changes between WT and *Col12a1* KO mice and p values are shown. Entities of the core matrisome (purple arrowheads) or of the matrisome associated cluster (gray arrowheads) are highlighted. P- values were adjusted using the Benjamini-Hochberg correction for multiple tests *, $p < 0.1$; **, $p < 0.05$, ***, $p < 0.01$; ****, $p < 0.001$.

(E) Differentially expressed genes of the core matrisome within the *Tnmd*+ subpopulation are shown in t-SNE plots.

that collagen XII is mainly expressed in cartilage, tendon and ligaments (see Figure 1). Patellar subluxation is highly likely to exert a major mechanical impact on the ECM organization of tendons and ligaments and therefore a differential expression and matrisome analysis.[13] Cross comparison analysis was performed

only for cells expressing *Tnmd* (Figure 5C, WT: 593 *Tnmd+* cells, *Col12a1* KO: 486 *Tnmd+* cells). In total, 33 genes were differentially expressed between cells isolated from WT or *Col12a1* KO mice including 8 core matrisome genes and 5 matrisome-associated genes (Figure 5D). We then focused the analysis on the core matrisome to understand the consequences of *Col12a1* deficiency for the structural organization of the ECM in tendon and ligaments. Four genes (*Col12a1*, *Kera*, *Spon2*, *Col11a2*) of the core matrisome were downregulated and four genes (*Tnn*, *Rspo2*, *Edil3*, *Ltbp2*) were upregulated in *Col12a1* KO compared to control. The *Col12a1* gene was the highest ranked downregulated gene of the core matrisome in the tenocyte population of the *Col12a1* KO mice. Of interest, mRNA levels of genes involved in collagen fibrillogenesis (*Col11a2*,[14] *Kera*[15,16]) and fibrosis (*Spon2*[17]) were decreased in the *Tnmd+* tenocyte cluster (Figure 5E). In contrast, mRNA levels of core matrisome genes regulating elastic-fiber organization (*Ltbp2*[18]), cell-matrix interactions (*Edil3*[19]; *Tnn*[20]) and Wnt signaling pathway activation (*Rspo2*[21]) were increased in the *Tnmd+* tenocyte cluster of *Col12a1* KO mice. This analysis showed that patellar subluxation in *Col12a1* KO mice is associated with the changes in gene signatures important for ECM formation, organization and recognition in tendon and ligaments.

Collagen XII deficiency is associated with a deformed or absent femoral trochlear groove in human patients

Our analysis highlights the importance of collagen XII for the organization of patella-tendon-ligament unit, but little is known about consequences of collagen XII deficiency for the knee joint organization in human patients. We therefore revisited the clinical files of two siblings (patient 1, patient 2) with a homozygous splicing mutation of *COL12A1* (c. 8006 + 1G>A). This mutation causes a skipping of exon 50 and a premature stop codon formation in exon 51, leading to a loss function because of truncated collagen XII translation without collagen domains.[8] In early childhood they had very unstable knees with patellar subluxations in both knees (Figures 6A and 6B). The X-ray analysis revealed for one sibling (patient 1) a complete absence of the femoral trochlear grooves, while these were less pronounced in the other (Figure 6A, left, lower panel). Moreover, the patella could not be kept in the proper position because of the missing femoral trochlear groove, was not well centered (upper panel) and located on the side of knee. In addition, we identified a novel homozygous mutation (c.5230 + 1G>A) in the *COL12A1* gene leading to recessive loss of collagen XII in one patient (patient 3). This patient presented with an autosomal recessive form of the collagen XII-associated myopathy without progressive muscle weakness, but with a remarkably small and dislocated patella and reduced femoral trochlear groove (Figures 6C and 6D). Finally, we revisited the MRI data of two patients (mother and daughter, patient 4, patient 5) with a heterozygous mutation (c.G8357A) in *COL12A1* gene causing a substitution of a conserved glycine residue in the Gly-X-Y motif of the triple helical domain of collagen XII.[6] Here, a flattened trochlear groove (Figure 6D), as well as joint hyperlaxity, jaw and hip dislocation was detected. The daughter's kneecaps were hypermobile and medially displaced upon adopting a standing position. Hence, malformed femoral trochlear grooves, patellar subluxation and joint destabilization are often clinical features in patients with recessive loss or heterozygous mutations of *COL12A1* gene.

DISCUSSION

Here, we report a novel function of collagen XII in the patella-tendon-ligament unit. We demonstrate that collagen XII is required to stabilize the patellofemoral joint and to maintain joint function in mice and in humans.

An interesting hallmark of *Col12a1* KO mice is the frequent dislocation of the patella. Because the femoral trochlear groove is not properly formed, the patella cannot be kept in the proper position and therefore easily slips to the side. At birth, 20% of the animals show this pathology, whereas upon increased physical activity during maturation up to 75% of the KO mice exhibit a patellar subluxation. Collagen XII has been described as a structural component of the ECM that organizes collagen fibrils[9] and may therefore provide a structural support for the femoral trochlear groove. Mechanical cues are also known to drive joint formation (for review see[22]) and, with lack of collagen XII, fibrils in the patella-tendon-ligament unit may not receive important mechanical signals to promote trochlear groove formation in the articular cartilage of the distal femur. In addition, collagen XII deficiency may directly affect the elasticity of tendons to provoke patellar subluxation. We previously described that lack of collagen XII results in irregular collagen fiber cross-sectional profiles and a significantly larger cross-sectional area in *flexor digitorum longus* tendons in *Col12a1* KO mice compared to WT animals.[23] We hypothesize that tendon flexibility is altered and these changes together with the absence of a femoral trochlear grooves may cause the dislocation of the patella

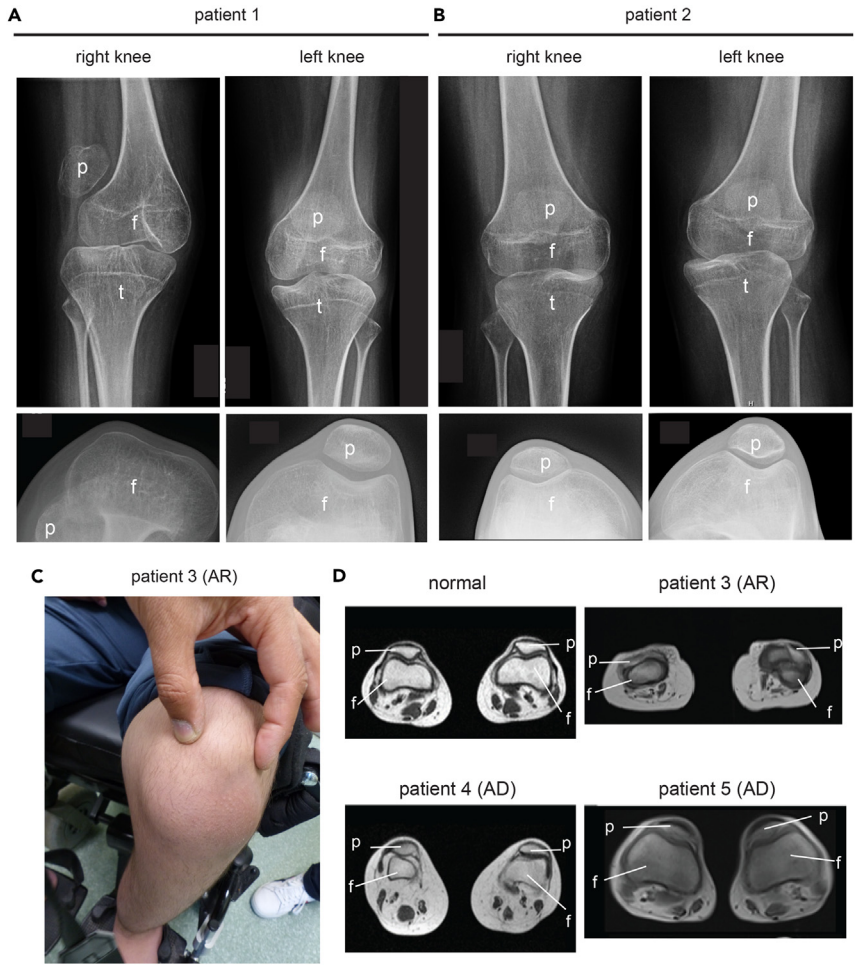

Figure 6. X-ray analysis of the human patella/knee region

(A and B) The knees of two *COL12A1* deficient siblings (1 + 2) with mutation of *COL12A1* c.8006 + 1G>A[8] were investigated by X-ray analysis. Frontal views reveal the localization of the patella (p), tibia (t) and femur (f) (upper panel). X-ray analysis of the bent knees to visualize the femoral groove and the patella (lower panel).

(C) Frontal view – knee from a homozygous patient (3) with an autosomal recessive mutation of *COL12A1*: c.5230 + 1G>A. Dislocation of the patella is indicated.

(D) Representative MRI-images of the malformed femoral groove in the novel patient (3) and in previously described autosomal dominant patients with mutation of *COL12A1*: G8357A (4 and 5) (Family 1a and 1b[6]) compared to normal. The position of femur (f) and patella (p) is indicated.

in collagen XII deficient mice and reduce resting muscle tonus and muscle length. Patellar subluxation occurs at late postnatal stages, when mobility increases, which shows the importance of mechanical forces for the development of the phenotype.

Tenocytes are the major cell type of tendons and we applied scRNA-seq technology to define the transcriptional response to collagen XII deficiency and changes in mechanical forces. Here, we identified a tenocyte population in a complex mixture of cells from whole hindlimb knee joint that can be used to define significant changes in the transcriptome of tenocytes from *Col12a1* KO mice. Of interest, we observed the regulation of ECM-related gene signatures in the tenocyte cluster. This demonstrates that changes in the ECM and the mechanical microenvironment of tendons from collagen XII deficient mice are sensed by tenocytes and translated into transcriptional responses. For the downregulated ECM-related genes a functional connection with collagen production and fibrillogenesis can be made. The profibrotic spondin 2 stimulates collagen secretion,[17] whereas the small leucine-rich proteoglycan keratocan (gene – *Kera*) is known to be expressed in cornea and tendon[15] and coordinates collagen fibril organization and packing in the corneal

stroma.[16] In addition, collagen XI controls fibril nucleation and assembly during tendon development.[14] The downregulation of these three genes together with the loss of collagen XII in the tenocyte cluster of *Col12a1* KO mice indicates a new molecular link between *Kera*, *Col11a2*, and *Col12a1* gene expression important for the organization and stabilization of collagen fibrils in tendon.

Since members of the small leucine-rich proteoglycan family, e.g., decorin, lumican, and fibromodulin, are known to influence the collagen fibril morphology, we compared our results to those from lumican and fibromodulin deficient animals. Lumican-deficient mice have collagen fibrils with increased diameter, forming a disorganized matrix in cornea and skin, with a consequent decrease in corneal clarity and increased skin laxity.[24] Fibromodulin-deficient mice have more immature, small diameter tendon collagen fibrils.[25] In comparison to *Col12a1* deficiency, double ablation of both the lumican and fibromodulin genes leads to strong Ehlers-Danlos syndrome phenotype. Unfortunately, the organization of the femoral trochlear groove was not studied in these mice, but a significant reduction in tendon stiffness and patellar subluxation was observed,[26] underlining the importance of tendon ECM composition for the function of the patellofemoral joint.

Other genes show an increased expression in the tenocyte cluster of *Col12a1* KO mice and these genes are linked to elastic fibril formation, cell matrix interactions and vascular remodeling. For example, *Ltbp2* may coordinate elastic fibril formation[18] and an increase in expression can have a direct impact on elastic fibers organization in tendon and ligaments of *Col12a1* KO mice. Moreover, genes mediating cell matrix interactions in periodontal ligaments (*Tnn*[20]) or during vessel remodeling are increased (*Edil3*[19,27]) and an activator of Wnt signaling in tendon progenitor cells (*Rspo2*[28]). This pathway can be critical for tendon repair processes after injury.[29] The regulation of these genes involved in ECM organization and Wnt signaling pathway activation may represent a damage response to pathological disorganization of the tendon ECM in *Col12a1* KO mice.

Of interest, patellar subluxation was associated with a significant quadriceps muscle mass reduction and a slight increase in the number of centralized nuclei in *Col12a1* KO mice. However, only <5% of the fibers have centralized nuclei and no fibrotic signs were visible in muscle sections. Progressive skeletal muscle phenotype as seen in other myopathy mouse models[30,31] is not seen. Muscle atrophy is a common consequence of injuries because of a lack of physical activity and impaired mobility. The quadriceps muscle requires an intact patellofemoral joint to transmit forces from femur to the tibia. We therefore hypothesize that the reduced quadriceps muscle mass is a direct consequence of impaired quadriceps activity because of a dysfunctional patellofemoral joint.

In human *COL12A1*-related mEDS both recessive and dominant modes of inheritance have been described.[7] Generally, recessively inherited, biallelic loss-of-function variants cause a severe congenital disease characterized by hypotonia, global muscle weakness and atrophy, as well as joint hyperlaxity.[8] In heterozygous patients, variants with a dominant-negative pathogenic effect on collagen XII fibrillar assembly have been described. These cause a much milder phenotype, characterized by motor developmental delay, proximal weakness, and joint hyperlaxity.[5,32] Ehlers-Danlos syndrome patients in general show joint dislocations and subluxations (partial dislocations) because of changes in elasticity. Our analysis of *COL12A1* patients now revealed novel morphological alterations of the femoral trochlear grooves, similar to those identified in *Col12a1* KO mice. In one instance the femoral trochlear groove was almost absent, whereas in the remaining knees the femoral trochlear groove seemed to be less pronounced than in unaffected individuals.

In summary, our results suggest that extracellular and cellular mechanisms mediated by collagen XII are important for the correct establishment of the tendon – patella – muscle unit in the knee joint of mice and humans and presumably many other joints. Findings in collagen XII deficient mice lead to the identification of a novel phenotype in human patients. The mouse phenotype-to-patient approach was very successful to define a common phenotype between species despite differences in mechanical loading of joints. Further mouse studies are warranted to elucidate the precise function of collagen XII in joints. Nevertheless, we provide evidence for the overall importance of collagen XII for joint stability and function and why joint hyperlaxity is observed in in human patients with mEDS.

Limitations of the study

In this study, we demonstrate the overall importance of collagen XII for the organization of the patellofemoral joint. Complex interactions between the ECM and cells translate changes into cellular responses,

but it is not clear whether the regulated genes directly contribute to the phenotype in mice and patients. Here we mainly focused on gene expression signatures, but how these regulated genes affect collagen assembly and tendon elasticity at the molecular levels needs further study. These regulated genes may elicit a tendon damage response to activate new progenitor cells for repair and to provide structural support for damaged fibrils. However, an snRNA-seq expression analysis can only provide an incomplete view of the molecular scenario. Collagen XII deficiency affects the organization of the ECM in the patellofemoral joint but is also important for osteoblast polarity and axonal guidance and regeneration. Therefore, defects in bone formation and musculoskeletal innervation may also contribute to the observed musculoskeletal phenotype. This interplay cannot be fully dissected in global *Col12a1* KO mice and tissue specific gene targeting studies are required to understand the tissue specific functions of collagen XII and the relation to the mEDS. So far, we have described the clinical phenotype of some patients with collagen XII deficiency, but further patients are need to define common clinical features of collagen XII deficiency in humans.

STAR★METHODS

Detailed methods are provided in the online version of this paper and include the following:

- KEY RESOURCES TABLE
- RESOURCE AVAILABILITY
  - Lead contact
  - Materials availability
  - Data and code availability
- EXPERIMENTAL MODEL AND STUDY PARTICIPANTS DETAILS
  - Animals
  - Human subjects
- METHOD DETAILS
  - Histology and immunohistochemistry
  - μCT analysis
  - Single-cell RNA-sequencing
- QUANTIFICATION AND STATISTICAL ANALYSIS
  - Differential expression and matrisome analysis of the single-cell RNA-sequencing dataset
  - Statistical evaluation of muscle fibres and *M. rectus femoris* organisation

SUPPLEMENTAL INFORMATION

Supplemental information can be found online at https://doi.org/10.1016/j.isci.2023.107225.

ACKNOWLEDGMENTS

We would like to thank the patient families for their participation and support of this research. In addition, we thank Semra Oezcelik and Christian Frie for excellent technical assistance.

This work was supported by the German Research Foundation (DFG) (AN: FOR2722-407176282/TP7 (AN1083/4-1), MP: FOR2722-407164210/TP3 (PA660/12-1), BB: FOR2722-407146744/TP1 (BR2304/12-1), 270922282 (BR2309/9-2), MK FOR2722-407164333/TP4 (KO2247/8-1), JSBMR Frontier Scientist Grant and the Morinaga Foundation For Health and Nutrition (YI) and by the European Union's Horizon 2020 research and innovation program under the Marie Sklodowska-Curie grant agreement No 721432 (GO, AP and BB).

AUTHORS CONTRIBUTIONS

Conceptualization, B.B., M.Z., and M.K. and Methodology, B.B., D.B., J.A., M.K., M.Z., and Y.I.; Investigation, A.N., A.P., F.M., G.S., J.B., J.H., M.H., M.Z., and T.I.; Visualization, A.N.; F.M., J.B., J.H., and M.H.; Data Curation, J.A., J.S., M.H., and V. S.; Writing – Original Draft, A.N., A.P., B.B., G.S., M.K., M.H., M.P., and M.Z.; Writing – Review and Editing, B.B., D.B., G.O., M.K., M.K.R., M.P., V.S., and Y.I.; Funding Acquisition, B.B., G.O., and M.K.; Resources, D.B. and G.S.; Supervision, A.P., G.O., M.P., M.K., and B.B.

DECLARATION OF INTERESTS

The authors declare no competing interests.

Received: August 4, 2022
Revised: May 5, 2023
Accepted: June 23, 2023
Published: June 28, 2023

REFERENCES

1. Chiquet, M., Birk, D.E., Bönnemann, C.G., and Koch, M. (2014). Collagen XII: Protecting bone and muscle integrity by organizing collagen fibrils. Int. J. Biochem. Cell Biol. *53*, 51–54. https://doi.org/10.1016/j.biocel.2014.04.020.

2. Veit, G., Hansen, U., Keene, D.R., Bruckner, P., Chiquet-Ehrismann, R., Chiquet, M., and Koch, M. (2006). Collagen XII interacts with avian tenascin-X through its NC3 domain. J. Biol. Chem. *281*, 27461–27470. https://doi.org/10.1074/jbc.M603147200.

3. Koch, M., Bohrmann, B., Matthison, M., Hagios, C., Trueb, B., and Chiquet, M. (1995). Large and small splice variants of collagen XII: differential expression and ligand binding. J. Cell Biol. *130*, 1005–1014. https://doi.org/10.1083/jcb.130.4.1005.

4. Yamagata, M., Yamada, K.M., Yamada, S.S., Shinomura, T., Tanaka, H., Nishida, Y., Obara, M., and Kimata, K. (1991). The complete primary structure of type XII collagen shows a chimeric molecule with reiterated fibronectin type III motifs, von Willebrand factor A motifs, a domain homologous to a noncollagenous region of type IX collagen, and short collagenous domains with an Arg-Gly-Asp site. J. Cell Biol. *115*, 209–221. https://doi.org/10.1083/jcb.115.1.209.

5. Mohassel, P., Liewluck, T., Hu, Y., Ezzo, D., Ogata, T., Saade, D., Neuhaus, S., Bolduc, V., Zou, Y., Donkervoort, S., et al. (2019). Dominant collagen XII mutations cause a distal myopathy. Ann. Clin. Transl. Neurol. *6*, 1980–1988. https://doi.org/10.1002/acn3.50882.

6. Hicks, D., Farsani, G.T., Laval, S., Collins, J., Sarkozy, A., Martoni, E., Shah, A., Zou, Y., Koch, M., Bönnemann, C.G., et al. (2014). Mutations in the collagen XII gene define a new form of extracellular matrix-related myopathy. Hum. Mol. Genet. *23*, 2353–2363. https://doi.org/10.1093/hmg/ddt637.

7. Delbaere, S., Dhooge, T., Syx, D., Petit, F., Goemans, N., Destrée, A., Vanakker, O., De Rycke, R., Symoens, S., and Malfait, F. (2020). Novel defects in collagen XII and VI expand the mixed myopathy/Ehlers-Danlos syndrome spectrum and lead to variant-specific alterations in the extracellular matrix. Genet. Med. *22*, 112–123. https://doi.org/10.1038/s41436-019-0599-6.

8. Zou, Y., Zwolanek, D., Izu, Y., Gandhy, S., Schreiber, G., Brockmann, K., Devoto, M., Tian, Z., Hu, Y., Veit, G., et al. (2014). Recessive and dominant mutations in COL12A1 cause a novel EDS/myopathy overlap syndrome in humans and mice. Hum. Mol. Genet. *23*, 2339–2352. https://doi.org/10.1093/hmg/ddt627.

9. Izu, Y., Sun, M., Zwolanek, D., Veit, G., Williams, V., Cha, B., Jepsen, K.J., Koch, M., and Birk, D.E. (2011). Type XII collagen regulates osteoblast polarity and communication during bone formation. J. Cell Biol. *193*, 1115–1130. https://doi.org/10.1083/jcb.201010010.

10. Fukusato, S., Nagao, M., Fujihara, K., Yoneda, T., Arai, K., Koch, M., Kaneko, K., Ishijima, M., and Izu, Y. (2021). Collagen XII Deficiency Increases the Risk of Anterior Cruciate Ligament Injury in Mice. J. Clin. Med. *10*, 4051. https://doi.org/10.3390/jcm10184051.

11. Encarnacion-Rivera, L., Foltz, S., Hartzell, H.C., and Choo, H. (2020). Myosoft: An automated muscle histology analysis tool using machine learning algorithm utilizing FIJI/ImageJ software. PLoS One *15*, e0229041. https://doi.org/10.1371/journal.pone.0229041.

12. Bubb, K., Holzer, T., Nolte, J.L., Krüger, M., Wilson, R., Schlötzer-Schrehardt, U., Brinckmann, J., Altmüller, J., Aszodi, A., Fleischhauer, L., et al. (2021). Mitochondrial respiratory chain function promotes extracellular matrix integrity in cartilage. J. Biol. Chem. *297*, 101224. https://doi.org/10.1016/j.jbc.2021.101224.

13. Hynes, R.O., and Naba, A. (2012). Overview of the matrisome–an inventory of extracellular matrix constituents and functions. Cold Spring Harb. Perspect. Biol. *4*, a004903. https://doi.org/10.1101/cshperspect.a004903.

14. Wenstrup, R.J., Smith, S.M., Florer, J.B., Zhang, G., Beason, D.P., Seegmiller, R.E., Soslowsky, L.J., and Birk, D.E. (2011). Regulation of collagen fibril nucleation and initial fibril assembly involves coordinate interactions with collagens V and XI in developing tendon. J. Biol. Chem. *286*, 20455–20465. https://doi.org/10.1074/jbc.M111.223693.

15. Zhang, Y., Kao, W.W.Y., Hayashi, Y., Zhang, L., Call, M., Dong, F., Yuan, Y., Zhang, J., Wang, Y.C., Yuka, O., et al. (2017). Generation and Characterization of a Novel Mouse Line, Keratocan-rtTA (KeraRT), for Corneal Stroma and Tendon Research. Invest. Ophthalmol. Vis. Sci. *58*, 4800–4808. https://doi.org/10.1167/iovs.17-22661.

16. Liu, C.Y., Birk, D.E., Hassell, J.R., Kane, B., and Kao, W.W.Y. (2003). Keratocan-deficient mice display alterations in corneal structure. J. Biol. Chem. *278*, 21672–21677. https://doi.org/10.1074/jbc.M301169200.

17. Rana, I., Kataria, S., Tan, T.L., Hajam, E.Y., Kashyap, D.K., Saha, D., Ajnabi, J., Paul, S., Jayappa, S., Ananthan, A.S.H.P., et al. (2023). Mindin (SPON2) Is Essential for Cutaneous Fibrogenesis in a Mouse Model of Systemic Sclerosis. J. Invest. Dermatol. *143*, 699–710.e10. https://doi.org/10.1016/j.jid.2022.10.011.

18. Adamo, C.S., Zuk, A.V., and Sengle, G. (2021). The fibrillin microfibril/elastic fibre network: A critical extracellular supramolecular scaffold to balance skin homoeostasis. Exp. Dermatol. *30*, 25–37. https://doi.org/10.1111/exd.14191.

19. Hidai, C., Kawana, M., Kitano, H., and Kokubun, S. (2007). Discoidin domain of Del1 protein contributes to its deposition in the extracellular matrix. Cell Tissue Res. *330*, 83–95. https://doi.org/10.1007/s00441-007-0456-9.

20. Imhof, T., Balic, A., Heilig, J., Chiquet-Ehrismann, R., Chiquet, M., Niehoff, A., Brachvogel, B., Thesleff, I., and Koch, M. (2020). Pivotal Role of Tenascin-W (-N) in Postnatal Incisor Growth and Periodontal Ligament Remodeling. Front. Immunol. *11*, 608223. https://doi.org/10.3389/fimmu.2020.608223.

21. Jin, Y.R., Han, X.H., Nishimori, K., Ben-Avraham, D., Oh, Y.J., Shim, J.W., and Yoon, J.K. (2020). Canonical WNT/beta-Catenin Signaling Activated by WNT9b and RSPO2 Cooperation Regulates Facial Morphogenesis in Mice. Front. Cell Dev. Biol. *8*, 264. https://doi.org/10.3389/fcell.2020.00264.

22. Pitsillides, A.A., and Ashhurst, D.E. (2008). A critical evaluation of specific aspects of joint development. Dev. Dyn. *237*, 2284–2294. https://doi.org/10.1002/dvdy.21654.

23. Izu, Y., Adams, S.M., Connizzo, B.K., Beason, D.P., Soslowsky, L.J., Koch, M., and Birk, D.E. (2021). Collagen XII mediated cellular and extracellular mechanisms regulate establishment of tendon structure and function. Matrix Biol. *95*, 52–67. https://doi.org/10.1016/j.matbio.2020.10.004.

24. Chakravarti, S., Magnuson, T., Lass, J.H., Jepsen, K.J., LaMantia, C., and Carroll, H. (1998). Lumican regulates collagen fibril assembly: skin fragility and corneal opacity in the absence of lumican. J. Cell Biol. *141*, 1277–1286. https://doi.org/10.1083/jcb.141.5.1277.

25. Svensson, L., Aszódi, A., Reinholt, F.P., Fässler, R., Heinegård, D., and Oldberg, A. (1999). Fibromodulin-null mice have abnormal collagen fibrils, tissue organization, and altered lumican deposition in tendon. J. Biol. Chem. *274*, 9636–9647. https://doi.org/10.1074/jbc.274.14.9636.

26. Jepsen, K.J., Wu, F., Peragallo, J.H., Paul, J., Roberts, L., Ezura, Y., Oldberg, A., Birk, D.E., and Chakravarti, S. (2002). A syndrome of joint

laxity and impaired tendon integrity in lumican- and fibromodulin-deficient mice. J. Biol. Chem. *277*, 35532–35540. https://doi.org/10.1074/jbc.M205398200.

27. Zhao, M., Zheng, Z., Li, C., Wan, J., and Wang, M. (2022). Developmental endothelial locus-1 in cardiovascular and metabolic diseases: A promising biomarker and therapeutic target. Front. Immunol. *13*, 1053175. https://doi.org/10.3389/fimmu.2022.1053175.

28. Tachibana, N., Chijimatsu, R., Okada, H., Oichi, T., Taniguchi, Y., Maenohara, Y., Miyahara, J., Ishikura, H., Iwanaga, Y., Arino, Y., et al. (2022). RSPO2 defines a distinct undifferentiated progenitor in the tendon/ligament and suppresses ectopic ossification. Sci. Adv. *8*, eabn2138. https://doi.org/10.1126/sciadv.abn2138.

29. Kishimoto, Y., Ohkawara, B., Sakai, T., Ito, M., Masuda, A., Ishiguro, N., Shukunami, C., Docheva, D., and Ohno, K. (2017). Wnt/beta-catenin signaling suppresses expressions of Scx, Mkx, and Tnmd in tendon-derived cells. PLoS One *12*, e0182051. https://doi.org/10.1371/journal.pone.0182051.

30. Doe, J., Kaindl, A.M., Jijiwa, M., de la Vega, M., Hu, H., Griffiths, G.S., Fontelonga, T.M., Barraza, P., Cruz, V., Van Ry, P., et al. (2017). PTRH2 gene mutation causes progressive congenital skeletal muscle pathology. Hum. Mol. Genet. *26*, 1458–1464. https://doi.org/10.1093/hmg/ddx048.

31. Meinen, S., Lin, S., Thurnherr, R., Erb, M., Meier, T., and Rüegg, M.A. (2011). Apoptosis inhibitors and mini-agrin have additive benefits in congenital muscular dystrophy mice. EMBO Mol. Med. *3*, 465–479. https://doi.org/10.1002/emmm.201100151.

32. Jezela-Stanek, A., Walczak, A., Łaźniewski, M., Kosińska, J., Stawiński, P., Murcia Pienkowski, V., Biernacka, A., Rydzanicz, M., Kostrzewa, G., Krajewski, P., et al. (2019). Novel COL12A1 variant as a cause of mild familial extracellular matrix-related myopathy. Clin. Genet. *95*, 736–738. https://doi.org/10.1111/cge.13534.

33. Bouxsein, M.L., Boyd, S.K., Christiansen, B.A., Guldberg, R.E., Jepsen, K.J., and Müller, R. (2010). Guidelines for assessment of bone microstructure in rodents using micro-computed tomography. J. Bone Miner. Res. *25*, 1468–1486. https://doi.org/10.1002/jbmr.141.

34. Pathan, M., Keerthikumar, S., Ang, C.S., Gangoda, L., Quek, C.Y.J., Williamson, N.A., Mouradov, D., Sieber, O.M., Simpson, R.J., Salim, A., et al. (2015). FunRich: An open access standalone functional enrichment and interaction network analysis tool. Proteomics *15*, 2597–2601. https://doi.org/10.1002/pmic.201400515.

35. Preibisch, S., Saalfeld, S., and Tomancak, P. (2009). Globally optimal stitching of tiled 3D microscopic image acquisitions. Bioinformatics *25*, 1463–1465. https://doi.org/10.1093/bioinformatics/btp184.

36. Charles, J.P., Cappellari, O., Spence, A.J., Hutchinson, J.R., and Wells, D.J. (2016). Musculoskeletal Geometry, Muscle Architecture and Functional Specialisations of the Mouse Hindlimb. PLoS One *11*, e0147669. https://doi.org/10.1371/journal.pone.0147669.

37. Brandau, O., Meindl, A., Fässler, R., and Aszódi, A. (2001). A novel gene, tendin, is strongly expressed in tendons and ligaments and shows high homology with chondromodulin-I. Dev. Dyn. *221*, 72–80. https://doi.org/10.1002/dvdy.1126.

38. Naba, A., Clauser, K.R., Ding, H., Whittaker, C.A., Carr, S.A., and Hynes, R.O. (2016). The extracellular matrix: Tools and insights for the "omics" era. Matrix Biol. *49*, 10–24. https://doi.org/10.1016/j.matbio.2015.06.003.

39. Etich, J., Koch, M., Wagener, R., Zaucke, F., Fabri, M., and Brachvogel, B. (2019). Gene Expression Profiling of the Extracellular Matrix Signature in Macrophages of Different Activation Status: Relevance for Skin Wound Healing. Int. J. Mol. Sci. *20*, 5086. https://doi.org/10.3390/ijms20205086.

STAR★METHODS

KEY RESOURCES TABLE

REAGENT or RESOURCE	SOURCE	IDENTIFIER
Antibodies		
Rabbit anti-collagen XII, KR33	Veit et al.[2]	RRID: AB_2801624
Goat anti-rabbit IgG(H+L), Cy3	Jackson ImmunoResearch	Cat# 111-165-144; RRID: AB_2338006
Chemicals, peptides, and recombinant proteins		
Bovine Serum Albumin	SERVA	Cat# 11924
Collagenase II	Worthington Biochemicals	Cat# LS004176 Lot# 41K21578 ACT 265U/mg
DAPI	Sigma-Aldrich	Cat# 32670
DMEM/F12	Thermo Fisher Scientific	Cat# 11320033
Ethylenediaminetetraacetic acid (EDTA)	Carl Roth	Cat# 8043.2
Fetal Bovine Serum	Biochrom	Cat# S0115
Hyaluronidase	Sigma-Aldrich	Cat# H3506
Iodine-potassium iodide solution	Sigma-Aldrich	Cat# L6146
10% Neutral-buffered formalin (NBF)	Sigma- Aldrich	Cat# HT501128
Mowiol 4-88	Calbiochem	Cat# 475904
Normal Goat Serum	Abcam	Cat# ab7481
Paraformaldehyde	VWR	Cat# 28794.295
Sodium acetate trihydrate	Merck	Cat# 1.06267.1000
Sodium monobasic phosphate dihydrate	VWR	Cat# 28011.291
Triton X-100	Sigma-Aldrich	Cat# T9284
Tween20	Sigma-Aldrich	Cat# P7949
Wheat Germ Agglutinin, Alexa 488 conjugated	Invitrogen	Cat# W11261
Deposited data		
Single cell RNA-seq data	this study	GEO: GSE234964
Experimental models: Organisms/strains		
Mouse C57BL6N/129JS2/SvPasCrl, *Col12a1* KO	Izu et al.[9]	N/A
Software and algorithms		
3D Gaussian filter algorithm	Bouxsein et al.[33]	https://www.scanco.ch/sw.html
Cell Ranger V7.0.0	10X Genomics	https://support.10xgenomics.com/single-cell-gene-expression/software/overview/welcome
CTVox	Bruker microCT	https://www.bruker.com/en/products-and-solutions/preclinical-imaging/micro-ct/3d-suite-software.html
Funrich V3.1	Pathan et al.[34]	http://www.funrich.org/
Graphpad 8.0	Graphpad	https://www.graphpad.com/
Grid/Collection stitching tool	Preibisch et al.[35]	https://imagej.net/plugins/image-stitching
ImageJ, Fuji Distribution	ImageJ	https://imagej.net/ij/index.html
Loupe Browser V6.2	10X Genomics	https://support.10xgenomics.com/single-cell-gene-expression/software/overview/welcome
NRecon	Bruker microCT	https://www.bruker.com/en/products-and-solutions/preclinical-imaging/micro-ct/3d-suite-software.html
Myosoft	Encarnacion-Rivera et al.[11]	https://bio.tools/myosoft

RESOURCE AVAILABILITY

Lead contact

Further information and requests for reagents should be directed to and will be fulfilled by the lead contacts, Bent Brachvogel (bent.brachvogel@uni-koeln.de).

Materials availability

This study did not generate new unique reagents.

Data and code availability

- Single-cell RNA-seq data have been deposited at Gene Expression Omnibus under accession number GSE234964. Microscopy data reported in this paper will be shared by the lead contact upon request.
- This study did not generate any original code.
- Any additional information required to reanalyze the data reported in this paper is available from the lead contact upon request.

EXPERIMENTAL MODEL AND STUDY PARTICIPANTS DETAILS

Animals

All animal experiments were performed in agreement with the guidelines of the German animal protection law (Institutional review board:"Landesamt für Natur, Umwelt und Verbraucherschutz Nordrhein-Westfalen"; AZ: 84-02.04.2019.A326). Animals were housed in a specific pathogen-free facility at 20 to 24°C on a 12 to 12 h light/dark cycle in individual ventilated cages and supplied with standard irradiated mouse chow and water *ad libitum*. *Col12a1* KO mice were generated from heterozygous breedings of mixed C57BL6/N and 129/SvJ background.[9] All mouse genotypes were determined by genotyping PCR using genomic DNA isolated from ear biopsies. Inbred sex matched littermates with genotype of WT and KO were randomly assigned to experiment groups. At P3, P7 and P12, both sexes were used. At the age of 1, 3, and 6 months, only female mice were used in the study.

Human subjects

Clinical features of knee joints in total 5 patients were described in this study, which were investigated in Klinikum Kassel, Germany and Newcastle University's John Walton Muscular Dystrophy Research Centre, UK. Patient 1 and 2 are two siblings (male, Turkish descent) with a homozygous recessive loss of *COL12A1* due to a mutation of the splice donor site of intron 50 causing a premature stop and the absence of the protein.[8] Both patients (now young adults) are not able to walk independently and require motorized wheelchairs. The myopathy did not progress since birth and remains stable. Since early on, both patients received night-time breathing support. They manage to change from a lying to a sitting position, but never to stand up by themselves. Due to scoliosis, both patients as teenagers required back surgery for stabilization. For patient data collection (patient 1 and 2) through the Center of Neuropaediatrics in the Klinikum Kassel, all subjects gave the appropriate permissions and consents.

The patient 3 (male, Pakistani descent) with the autosomal recessive form of the collagen XII-associated myopathy with the homozygous mutation (c.5230+1G>A) and recessive loss of *COL12A1* presented as a floppy baby with poor muscle bulk, distally more than proximally. He had micrognathia with open-mouthed breathing, rocker bottom feet, protruding calcanei and a prominent occiput. The patient never managed to walk independently and is wheelchair bound. He has developed a scoliosis without signs of progressive muscle weakness. The patient 4 and 5 (female, white British descent) with a heterozygous mutation causing a substitution of a conserved glycine residue in the Gly-X-Y motif of the triple helical domain of collagen XII, developed kyphosis and a severe atrophy of the *M. rectus femoris* muscle.[6] Patient data collection (patient 3, 4 and 5) through Newcastle University's John Walton Muscular Dystrophy Research Centre was approved by the research ethics committee (REC: 16/EE/0076; MR imaging in genetic muscle disease). All objects gave the appropriate permissions and consents.

METHOD DETAILS

Histology and immunohistochemistry

Paraffin sections

Right hindlimb knee joints of *Col12a1* KO mice and littermate WT controls were collected at the indicated time points (for animals aged under 1 month, both sexes were used; for animals aged over 1 month, only female mice were used). They were fixed immediately in 4 % paraformaldehyde (w/v in PBS, pH = 7.4) for 24 h after collection. Decalcification was carried out in 0.5 M EDTA (pH = 8.0) at 4°C for 2 weeks with mild agitation. Samples were embedded in paraffin and sectioned by microtome (Leica Biosystem, Germany) at the thickness of 7 μm. After deparaffinization, Hematoxylin-Eosin and Alcian Blue staining was performed for histomorphological analysis. Immunofluorescent staining of collagen XII on paraffin sections was performed as follows: after deparaffinization, samples were treated with 5 mg/ml hyaluronidase (H3506, Sigma-Aldrich) in 0.1 M NaH_2PO_4/0.1 M sodium acetate (pH = 5.0) at 37°C for 30 minutes. Then slides were washed three times in TBS and incubated in 0.25% Triton X-100 (v/v in TBS, pH = 7.4) for 10 minutes at room temperature for permeabilization. After another three times TBS washing, blocking was conducted at room temperature for 45 minutes with 10% FBS, 5% NGS (v/v in TBS, pH = 7.4). Rabbit anti collagen XII antibody KR33 was diluted 1:1000 in 5% FBS (v/v in TBS, pH = 7.4) and incubated at 4°C overnight. The next day, sections were washed three times in TBS and incubated with secondary antibody conjugated to Cy3 diluted 1: 800 in 1% FCS/5% NGS (v/v in TBS, pH = 7.4) for 1 h at room temperature. After another three times washing in TBS, nuclear staining was performed by applying DAPI (1:100 in TBS, 32670, Sigma) at room temperature for 5 minutes. All slides were embedded in Mowiol mounting medium and analysed by fluorescence microscopy (Nikon Europe Eclipse TE2000-U microscope).

Cyrosections

Gastrocnemius and quadriceps muscles from 6 months old female WT and *Col12a1* KO mice were dissected and immediately snap-frozen in cold isopentane. Samples were stored at -80°C until sectioning. Muscle samples were sectioned with a cryostat (Leica, Germany) at a thickness of 7 μm and captured with Superfrost Plus adhesive microscopy slides (H867.1, Carl Roth, Germany). Hematoxylin-Eosin staining was performed according to standard methods. For the immunostaining, the slides were fixed for 10 minutes with 4 % paraformaldehyde (w/v in PBS, pH = 7.4), permeabilized for 10 minutes with 0.3% Tween20 (v/v in PBS, pH = 7.4) in room temperature and stained with rabbit anti collagen XII antibody KR33 (1:200 in 5 % FBS) followed by corresponding secondary antibodies coupled to Cy3 (1:800; Jackson ImmunoResearch) or Alexa 488 conjugated wheat germ agglutinin (WGA) (Invitrogen, 1:500) overnight at 4°C. Nuclear staining was performed by applying DAPI (1:100 in TBS, 32670, Sigma) at room temperature for 5 minutes. Slides were embedded in Mowiol mounting medium and analysed by fluorescence microscopy (Nikon Europe Eclipse TE2000-U microscope).

μCT analysis

For I_2KI-enhanced μCT scanning, a protocol[36] was adapted as follows: hindlimb knee joints of P7 mice from both sexes were collected and frozen in -80°C immediately after sacrifice. The hindlimb knee joints were then thawed and placed in 10% neutral-buffered formalin (NBF) (HT501128-4L, Sigma) for 24 h at 4°C under constant rotation for soft tissue fixation. Then samples were washed in PBS for 1 h to remove residual fixative. Samples were first scanned in a SkyScan 1172 system (Bruker microCT, Belgium) with source settings of at 50 kV, 200 μA, and a 960 ms exposure time and a pixel size of 4.98 μm using an Aluminium 0.5 mm filter. After CT scanning, the specimens were immersed in iodine-potassium iodide solution (I_2KI, Lugol's solution, L6146, Sigma) for 8 days to enhance soft tissue contrast, and placed in 70% ethanol until the next μCT scanning using the SkyScan 1172 system at the following settings: 60 kV, 167 μA, 4.98 μm resolution, Aluminium 0.5 mm filter and 960 ms exposure time. The images were reconstructed using NRecon software (Bruker microCT, Belgium), whereas volume renderings were constructed using CTvox software (Bruker microCT, Belgium). For μCT scanning, right hindlimb knee joints from 1 month old female mice were isolated, immediately fixed in 70% EtOH and stored in 4°C. Knee joints were evaluated using a high-resolution μCT scanner (μCT 35; Scanco Medical AG) and were scanned with an isotropic voxel size of 6 × 6 × 6 μm using 70-kVp tube voltage, 114-μA tube current, and 400 ms integration time. Image noise was removed by preprocessing of the grayscale data of the raw CT images using a 3D Gaussian filter algorithm and separation of mineralized tissue from the soft tissue by a global threshold of 200.

Single-cell RNA-sequencing

Hindlimb knee joints of P7 mice of both sexes were isolated WT and *Col12a1* KO mice, skin and paws were removed. Then they were digested in 4 mg/mL collagenase II (Worthington, USA) in DMEM/F-12 (supplied with 10% FBS) for 6 hours. After digestion, isolated cells were passed through 100 μm and 40 μm cell strainers (BD Bioscience, USA) to obtain single cell suspensions. Cells were washed three times with 0.04 % bovine serum albumin (Serva Electrophoresis GmbH, Germany) (v/v in PBS, pH = 7.4) by centrifugation at 400 g for 5 minutes and brought to a density of 1,000 cells / μL. Cell viability (> 90 %) was confirmed by 0.4 % trypan blue staining prior to processing according to 10x Genomics Chromium Single Cell 3' Reagent Kit User Guide (V3.1) as previously described.[12] Briefly, approximately 5,000 (1st experiment) or 10,000 cells (2nd experiment) of each genotype were loaded into Chromium Next gel beads in emulsion (GEMs) Chip G and single cell capture was performed with 10X Chromium Controller (10x Genomics). cDNA generation and library was prepared and 10μl of the cDNA solution was used (10× Genomics protocol) to create an Illumina library (P5 and P7 adapters for 3'mRNA) for sequencing (Illumina NovaSeq6000 systems). Reads were aligned, feature-barcode matrices were generated and data sets from two independent experiments (1st experiment 1xWT vs 1x *Col12a1* KO samples; 2nd experiment 2x WT vs 2x *Col12a1* KO samples) were merged (Cell Ranger software, V7.0.0, 10X Genomics). The data set was imported and analyzed by Loupe Browser (V6.2, 10X Genomics, see also Figure S5). Cluster annotation by cell type specific marker gene expression[12] was used to identify *tenomodulin* (*Tnmd*+) tenocytes-like cells[37] within the dataset for differential gene expression analysis.

QUANTIFICATION AND STATISTICAL ANALYSIS

Differential expression and matrisome analysis of the single-cell RNA-sequencing dataset

Fold change and false discovery rate adjustment by the Benjamini-Hochberg procedure was used to define differentially expressed mRNAs between WT and *Col12a1* KO *Tnmd*+ tenocytes-like cells in single cell RNA sequencing analysis. The entity lists of differentially expressed entities were exported to generate graphical representations as Venn diagrams using the FunRich V3.1 tool[34] and the matrisome database 2.0 (http://matrisomeproject.mit.edu)[38] as described previously.[39]

Statistical evaluation of muscle fibres and *M. rectus femoris* organisation

Muscle fiber

Whole muscle sections stained with DAPI and WGA were stitched together with the Grid/Collection stitching tool[35] in the Fiji/ImageJ software (National Institutes of Health) and the number of central nuclei was counted by the cell counter tool in Fiji/ImageJ (Figure 3D). In addition, the myosoft tool[11] was used to calculate the number of muscle fibres and the minimal Feret's diameter. Statistical significance between groups was calculated by unpaired two-tailed Student's t test and error bars are given as mean ± SD using the graphpad prism software 8.0. *, $p < 0.05$; **, $p < 0.01$, ***, $p < 0.001$.

M. rectus femoris

The CTAn software (Bruker, Belgium) was used to analyse micro-CT tomograms and the resultant 2D μCT morphometric data was used to produce 2D analytical profile graphs and heatmaps within RStudio (RStudio: Integrated Development for R. RStudio, PBC). An unpaired two-tailed Student's t test was applied for *M. rectus femoris* length and volume, error bars are given as mean ± SD using the graphpad prism software 8.0. ***,$p < 0.001$; as well as to compare means between WT and *Col12a1* KO groups along the length of the Lugol's stained rectus. Graphical heatmap illustrates statistical differences, error bars are given as mean ± SEM, red $p \leq 0.000\text{-}0.001$, yellow $p \leq 0.001\text{-}0.01$, green $p \leq 0.01\text{-}0.05$ and blue $p \geq 0.05$.